POLITECNICO DI TORINO
Repository ISTITUZIONALE

OPTIMAL PITCH MAP GENERATION FOR SCANNING PITCH DESIGN IN SELECTIVE SAMPLING

Original
OPTIMAL PITCH MAP GENERATION FOR SCANNING PITCH DESIGN IN SELECTIVE SAMPLING / Vezzetti, Enrico. - In: ROBOTICS AND AUTONOMOUS SYSTEMS. - ISSN 0921-8890. - (2009), pp. 578-590. [10.1016/j.robot.2009.02.003]

Availability:
This version is available at: 11583/1918401 since:

Publisher:
ELSEVIER

Published
DOI:10.1016/j.robot.2009.02.003

Terms of use:

This article is made available under terms and conditions as specified in the corresponding bibliographic description in the repository

Publisher copyright

(Article begins on next page)

12 October 2024

NOTICE: this is the author's version of a work that was accepted for publication in "ROBOTICS AND AUTONOMOUS SYSTEMS". Changes resulting from the publishing process, such as peer review, editing, corrections, structural formatting, and other quality control mechanisms may not be reflected in this document. Changes may have been made to this work since it was submitted for publication. A definitive version was subsequently published in ROBOTICS AND AUTONOMOUS SYSTEMS, Volume 57 Issue 6-7, June, 2009, Pages 578–590, DOI: 10.1016/j.robot.2009.02.003.

OPTIMAL PITCH MAP GENERATION FOR SCANNING PITCH DESIGN IN SELECTIVE SAMPLING

E. Vezzetti

Dipartimento di Sistemi di Produzione Ed Economia dell'Azienda, Politecnico di Torino, Corso Duca degli Abruzzi 24, 10129,Torino, Italy

Tel.: +39 011 5647294; Fax: +39 011 5647299; e-mail: enrico.vezzetti@polito.it

Abstract

Reverse engineering process represents one of the most known methodologies for creating 3D virtual models starting from physical ones. Even if in the last few years its usage has significantly increased, the remarkable involvement of the operator has until now represented a significant constraint for its growth. Having regard to the fact that this process, and in particular its first step, (that is the acquisition phase) strongly depends on the operator's ability and expertise, this paper aims at proposing a strategy for automatically supporting an "optimal" acquisition phase. Moreover, the acquisition phase represents the only moment in which there is a direct contact between the virtual model and the physical model. For this reason, designing an "optimal" acquisition phase will provide as output an efficient set of morphological data, which will turn out to be extremely useful for the following reverse engineering passages (pre-processing, segmentation, fitting, …). This scenario drives the researcher to use a selective sampling plan, whose grid dimensions are correlated with the complexity of the local surface region analyzed, instead of a constant one. As a consequence, this work proposes a complete operative strategy which, starting from a first raw preliminary acquisition, will provide, a new selective sampling plan during the acquisition phase, in order to allow a deeper and more efficient new scansion. The proposed solution does not require the creation of any intermediate model and relies exclusively on the analysis of the metrological performances of the 3D scanner device and of the morphological behaviour of the surface acquired.

Keywords: Reverse Engineering, Sampling Strategy, Scanner Uncertainty, Free-Form

1. Introduction

The Reverse engineering process starts from the usage of a scanning device which usually provides a "point cloud", that is a particular set of points describing a discrete sample of a physical model surface. The following steps are usually carried out by using the Delaunay's approach, which is simply a triangulation technique used to generate a polyhedral model of a physical one starting from a point cloud.

These are only two of the steps which form the reverse engineering process. This process starts from the point cloud acquisition to arrive at the virtual model reconstruction. It can be characterised by many possible settings and choices, which are sometimes quite difficult to define and which may possibly cause significant inconsistencies between the scanned sample region and the real surface.

One of the most common sources of errors is undoubtedly the 3D scanning device. Being a real measuring tool, The 3D scanner is likely to be affected by measurement uncertainty; that is why its outputs, which are usually represented by point clouds, often introduce anomalies which do not belong to the original shape and that are usually defined as "noise".

This “noise” is normally removed during the phase which follows the acquisition one and which consists of two different steps: the “pre-processing” step and the “segmentation” step, in which the points cloud is divided into several different sub-domains and patch surfaces [1].

The efficiency of the “pre-processing” step and of the “segmentation” stage strongly depends on the initial characteristics of the point cloud, and in particular on the number of points and on their placement in the Cartesian space. For this reason, it is necessary to provide a point data set (known as “selective sample”) already during the acquisition phase. Besides, this “selective sample” must be strictly correlated with the morphological characteristics of the original scanned surface.

In order to provide an efficient “selective sample”, it is important to remember that most 3D Scanners acquire the object surface by using a constant grid, whose dimensions depend on the technology (contact or non-contact) employed [2]. When working on a wide range of possible surface morphologies, the use of the above mentioned constant grid is likely to give rise to one of the two following scenarios: the generation of a too scattered points cloud, which would not be suitable for working on complex zones, or the formation of a plane, cylinder or cone-like scanning area, whose high resolution performances would be redundant.

Having regard to the falseness of the common assumption that “the database quality improving goes always together with the sampled points density”, it is possible to state that a sample grid crowded with too many points and obtained from a relatively simple surface, increases the uncertainty propagation, whose presence is normally due to the measuring tools. It is therefore possible to make a new assumption that “the database quality improving is directly proportional to the propriety of the points of the cloud”.

Hence, considering that the acquired point density depends on the scanning resolution, (whose value varies locally depending on the surface morphological complexity), the selective sampling approach may be obtained by involving an “expert” operator for deciding which is the best pitch to be locally employed. However, in this case, the whole process would be expected to be extremely time-consuming because of the possible iterations, and its final result would probably be highly subjective.

On the other hand, the whole process could be automated by employing a morphological descriptor parameter associated with the optimal point density (or scanning pitch). It would be theoretically possible to start from a preliminary acquired point set, characterized by a constant resolution, and then to perform and manage an automatic point cloud optimization in order to provide a new, more efficient plan (defined in terms of new point number and locations) for the new scanning session (Fig.1).

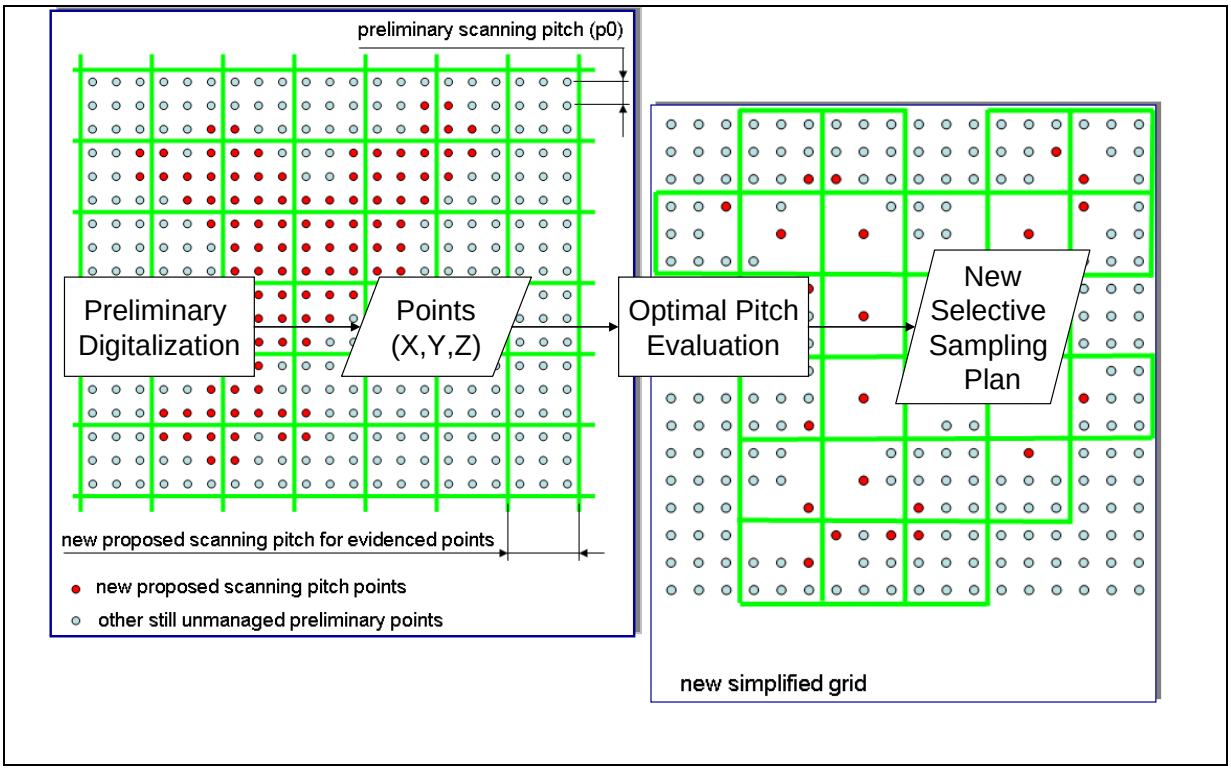

Figure 1: general description of the selective sampling concept

2. Technical literature

Even though, at present, the standard approach used during the 3D scanner acquisition is still principally handmade and driven by the operator expertise, some efforts have been made in the direction of an automatic methodology. However, most of the works already developed on the study of a selective acquisition pitch [5,6,7,8] have been developed not for reverse engineering purposes, but rather for computer inspection operations, which are often implemented with the availability of CAD models.

One of the most original solutions [9,10] developed for inspection purposes suggests an interesting strategy for selecting the distribution of discrete data points on sculptured surfaces. This strategy is based on the surface curvature and consists of a two-step surface subdivision stage. During the first step, the surface is uniformly divided into several smaller regions, which, during the second step, are in turn divided into even smaller sub-regions. The surface mean curvature is then calculated thanks to a uniform grid of points displaced on each of the sub-regions, which are subsequently ranked according to their average curvature values.

While these previously developed inspection strategies work on differentiable geometries, the new methodology described in this paper is based only on a preliminary raw point cloud, and on no other mathematical model. The main goal of this new methodology is to design a selective sampling plan able to provide a well organised point cloud in order to efficiently support the surface fitting step.

3. Optimal pitch map design strategy description

The Gaussian curvature has proved to be a good parameter for describing the local morphological

surface complexity, because of its “intrinsic” behaviour. (that is, it does not depend on the particular direction of the surface analysis) [11].

The Gaussian curvature approach for differentiable surfaces can be easily extended to point cloud analysis by using a triangulated model. Thanks to the Gauss-Bonnet theorem, the discrete Gaussian curvature can be easily calculated, since it is given by the angular excess of each one of the triangulated neighbourhoods, which have been previously generated through the Delaunay’s approach.

The Gaussian discrete parameter provides an intrinsic curvature value which enable the operator to assess the discrepancy between the actual local geometry and the planar one by employing the following formula:

$$K = 2\pi - \sum_i \vartheta_i \ , \ i = 1,...n \ , \qquad (1)$$

where K represents the Gaussian curvature value. This curvature value is calculated for each discrete neighbourhood, that is for each triangle, individuated through the index i, and sharing the central node with the other triangles. It is important to notice that there are as many triangulated neighbourhoods as there are points in the point cloud. For this reason, each point can be “labelled” with a specific curvature value (Fig.2).

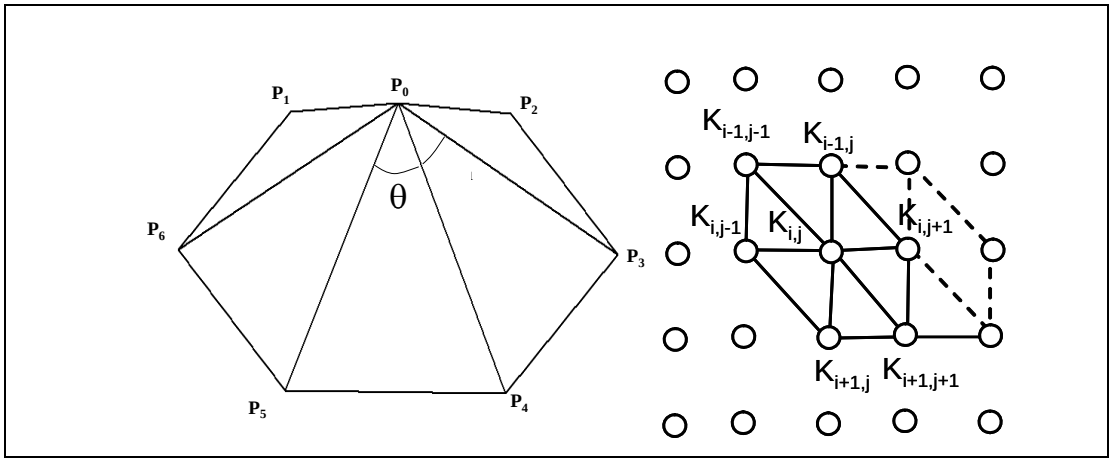

Figure 2: graphical representation of curvature *K* evaluation

Thanks to this procedure, it will be possible to associate to every point cloud a database composed by the preliminary points’ Cartesian coordinates (Fig.3a) and by the corresponding Gaussian discrete curvature values (“curvature map”) (Fig.3b).

Hence, taking into accounts that the curvature map reflects the morphological complexity of the preliminary sample and that the point density is proportional to the curvature value, it can be stated that it is possible to create an operative automatic approach by translating the curvature map into an “optimal pitch map”, which can subsequently be employed for a new scanning session.

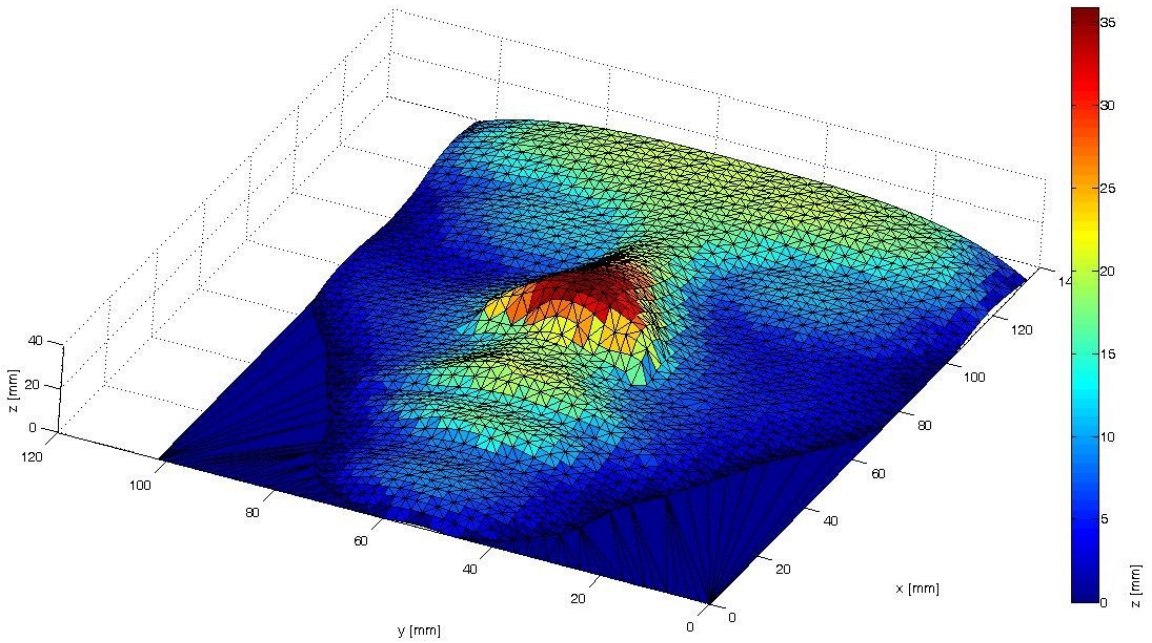

(a)

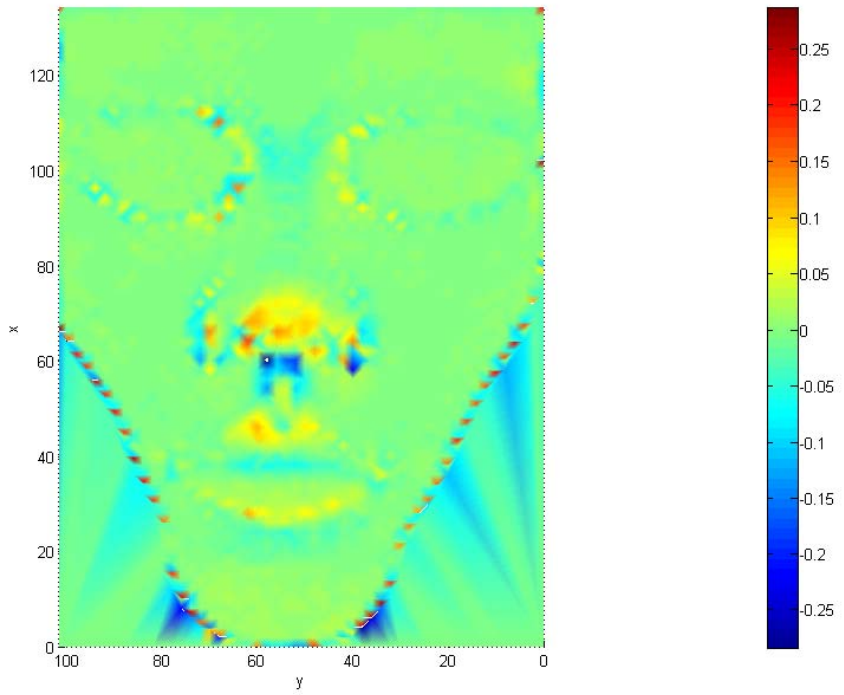

(b)

Figure 3: a) geometrical representation of a scanned surface (*the colour-map describes z coordinate values [mm]*); b) curvature map for the same surface (*the colour-map describes curvature K values*)

3.1 Free-Form and "disturbance" codification

In order to obtain an optimal pitch map and before describing in detail the methodology proposed thereof, it is necessary to make some considerations on the Free-Form concept.

The preliminary point cloud, which corresponds to an infinite population of points, can be considered as a sample obtained from several different differentiable surfaces. Furthermore, the point set cannot be considered as directly derived from an ideal free-form surface, characterized by shape smoothness and differentiability. In fact as it has been verified through several free-form geometries previously acquired, preliminary point clouds tend to show significant anomalous Gaussian curvature values. This fact suggests the presence of a particular portion of morphological complexity, which cannot properly be defined as "free-form", and which affects even the smoothest surfaces. In this paper this anomalous portion will be referred to as "disturbance".

From a physical point of view, the presence of this "disturbance" can be justified by the fact that the original surface is usually a real object surface, which has been previously scanned and which is therefore affected by a great number of anomalies. Examples of such anomalies are: sharp profiles and edges, (which, however, designers could have foreseen during the modelling steps), wrinkled surfaces and uncertainty contributes due to the manufacturing process, and finally an uncertainty rate related to the measuring devices being used. For this reason, a point cloud obtained through the acquisition of a free-form surface cannot be

considered as a “true” ideal “free-form” surface, but more properly as a sort of “free-shape”, containing both the features of the ideal “free-form” geometry and the characteristics of what has been previously defined as “disturbance” (Fig.4).

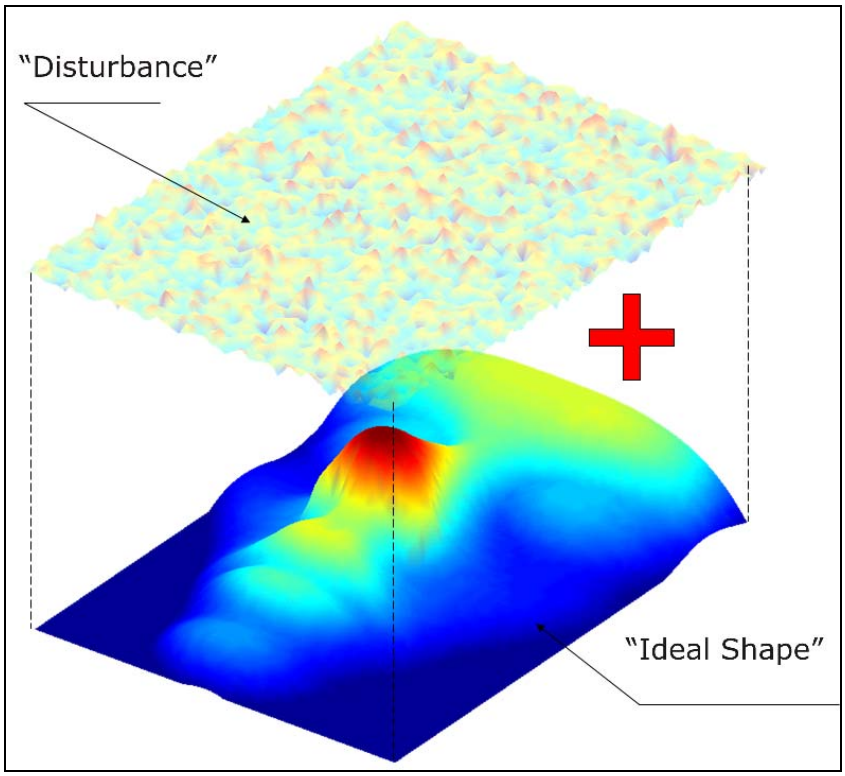

Figure 4: free shape concept: it means that the geometrical description of the surface, together with its descriptor (curvature *K*), is composed both by an ideal component and by a disturbance one.

The so-called “disturbance” is the aggregate of all those features which are related to morphological complexity but which do not suit the classical free-form definition. It is important to notice that these features cannot simply be classified as “noise”; instead, they are likely to include significant geometrical characteristics, such as scratches or dents which are necessary to implement a high quality control process. Therefore, it is possible to state that “disturbance” features are extremely useful to provide a more reliable description of such details (they allow the use of a higher number of points), and to improve the sample efficiency of the original surface description.

3.2 The pulse model: probability density functions for “disturbance” and curvature pitch function

Several experimental tests developed on benchmarking surfaces have shown that, when working with significant anomalous dimensions and intensities, the “disturbance” contribution is likely to hide the ideal free-form shape curvature value. In these cases, which are rather frequent, surfaces showing a completely different curvature behaviour, (for instance a simple plane compared to a properly defined Free-Form surface), may show very similar Gaussian curvature sampled frequencies, and also the same Gaussian curvature standard deviation s_K .This is due to the fact that both surfaces have the same statistical noise.

These scenarios suggest that the “disturbance” usage can be approximately modelled as a random pulse

function along the z-axis. This function shall be characterized by normal distribution, zero average, and assigned standard deviation s_I. If such a disturbance model is applied to a simple plane instead of a more complicated surface (in order to simplify calculations), it is possible to obtain a specific formula for Gaussian curvature calculation.

Starting from the curvature K formula (1) and considering a different formalisation, it is possible to obtain the following result by introducing the coordinates of the boundary vertex neighbourhood:

$$K_t = 2\pi - \sum_{i=1}^{n} \arccos\left\{ \frac{\{(x_i - x_0) \quad (y_i - y_0) \quad (z_i - z_0)\}^T \{(x_{i+1} - x_0) \quad (y_{i+1} - y_0) \quad (z_{i+1} - z_0)\}}{\left|\{(x_i - x_0) \quad (y_i - y_0) \quad (z_i - z_0)\}\right| \cdot \left|\{(x_{i+1} - x_0) \quad (y_{i+1} - y_0) \quad (z_{i+1} - z_0)\}\right|} \right\} \tag{2}$$

where (x_0,y_0,z_0) represents the central node coordinates and (x_i,y_i,z_i) represents the boundary vertexes. The curvature value corresponding to each of the four-boundary vertex neighbourhoods and related to the central node of the same neighbourhood will be calculated as follows:

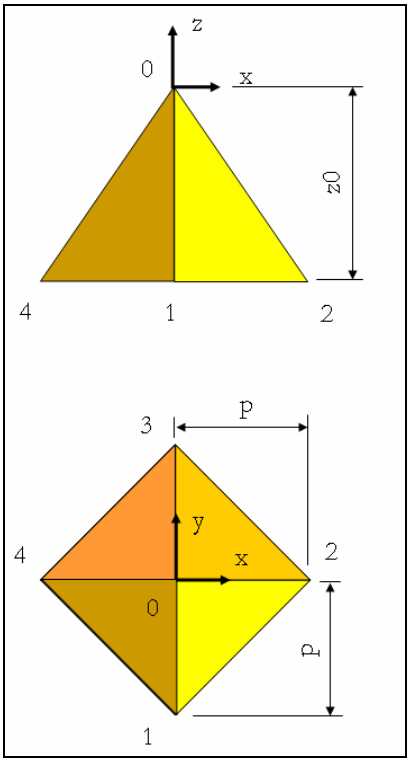

Figure 5 : four-boundary vertex neighbourhood

$$K = 2\pi - \sum_{i=1}^{n} \arccos(\ldots) = 2\pi - 4 \cdot \arccos\left(\frac{\{0 \quad -p \quad -z_0\}^T \{p \quad 0 \quad -z_0\}}{\left(p^2 + z_0^2\right)} \right) = 2\pi - 4 \cdot \arccos \frac{z_0^2}{p^2 + z_0^2} \tag{3}$$

Furthermore, when working on a plane (Fig.6), if I is, for instance, assumed to be the normally distributed pulse intensity, the curvature K formulation will be:

$$K(I) = 2\pi - 4\arccos\left(\frac{I^2}{{p_0}^2 + I^2}\right). \qquad (4)$$

where p_0 stands for the preliminary scanning pitch, and I indicates the intensity of the pulse function along the z-axis, which signals the presence of a certain amount of disturbance all over the sampled surface. Furthermore, the curvature model (4) can be used to define a "curvature probability density function", whose shape and continuity depend on the statistical definition of the "disturbance".

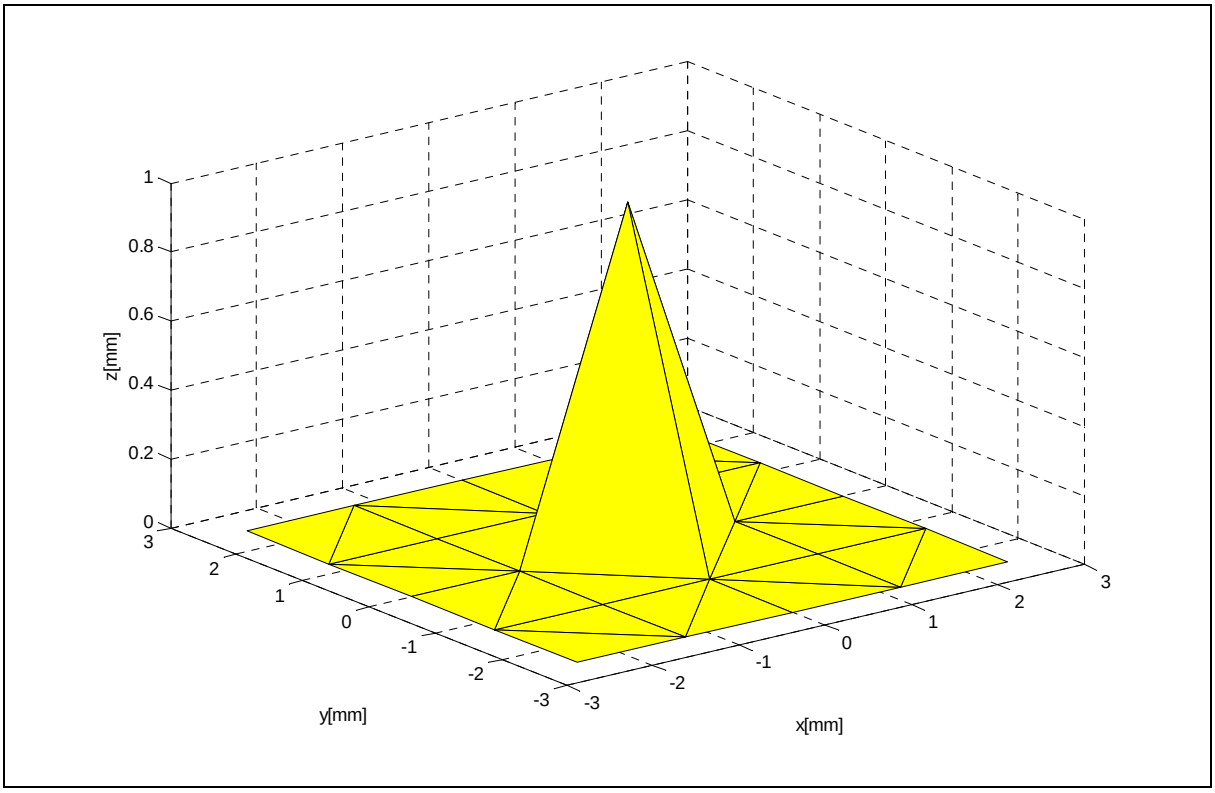

Figure 6: plane with a single perturbed point

As It has previously been said, the "disturbance" along the z-axis has been supposed to be characterized by a simple normal distribution with zero average. The statistical analysis offers a theorem [12] for random variable changing, which allows to combine Eq.(4) with the normal distribution of the "disturbance" I:

$$f(I) = \frac{1}{\sqrt{2\pi}\, s_I} e^{\left(\frac{I^2}{2s_I^2}\right)}, \qquad \text{probability density function of the "disturbance" } I\text{, along the } z\text{-axis;} \qquad (5)$$

Starting from the previous $K(I)$ formula (4) and evaluating the disturbance intensity I, it is possible to obtain the following representation:

$$I(K) = p\sqrt{\frac{\cos\left(\frac{2\pi - K}{4}\right)}{1-\cos\left(\frac{2\pi - K}{4}\right)}} = p\sqrt{\frac{\sin\left(\frac{K}{4}\right)}{1-\sin\left(\frac{K}{4}\right)}} \tag{6}$$

Hence, if the formula (5) is expressed as a K function, by introducing equation (6) into equation (5), it is possible to obtain the following formulae:

$$f\ \left(I(K)\right) = \frac{1}{\sqrt{2\pi}s_I} e^{-\frac{1}{2}\frac{p^2}{s_I^2}\frac{\sin(K/4)}{[1-\sin(K/4)]}} \tag{7}$$

However, in order to provide an operative procedure, it is also necessary to introduce another expression, where p_0 represents the preliminary pitch:

$$\frac{d}{dK} I(K)\Big|_{p=p_0} = \frac{p_0}{8}\frac{\cos\left(\frac{K}{4}\right)}{\sqrt{\sin\left(\frac{K}{4}\right)}\left(1-\sin\left(\frac{K}{4}\right)\right)^{3/2}} \tag{8}$$

Taking into account the previous expressions and applying the random variable transformation theorem [12], it is possible to prove that if X is a continuous random variable with density function $f_X(X)$, then the variable $Y = g(X)$ will have the same continuum and will be characterised by the following density function:

$$f_Y(Y) = \left|\frac{d}{dY} g^{-1}(Y)\right| f_X\left(g^{-1}(Y)\right) \tag{9}$$

This is due to the fact that $Y = g(X)$ is a function which defines a bi-univocal transformation between D_X and D_Y and that $\frac{d}{dY} g^{-1}(Y)$ is a continuous variable which differs from zero for every $Y \in D_Y$.

Hence, by introducing formulae (7) and (8) into the just mentioned formula (9) , it is possible to obtain the following formula:

$$f(K) = \left|\frac{d}{dK} I(K)\right| f(I(K)), \tag{10}$$

If the above reasoning is extended to curvature K negative values, it is then possible to demonstrate that even an expected value equal to zero is related to this particular statistical distribution (Fig.7)

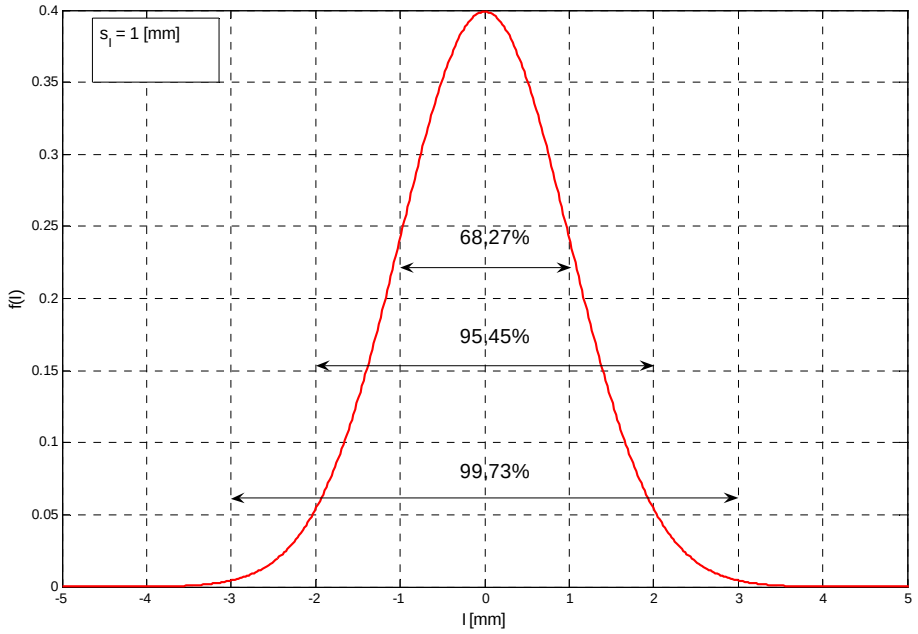

(a)

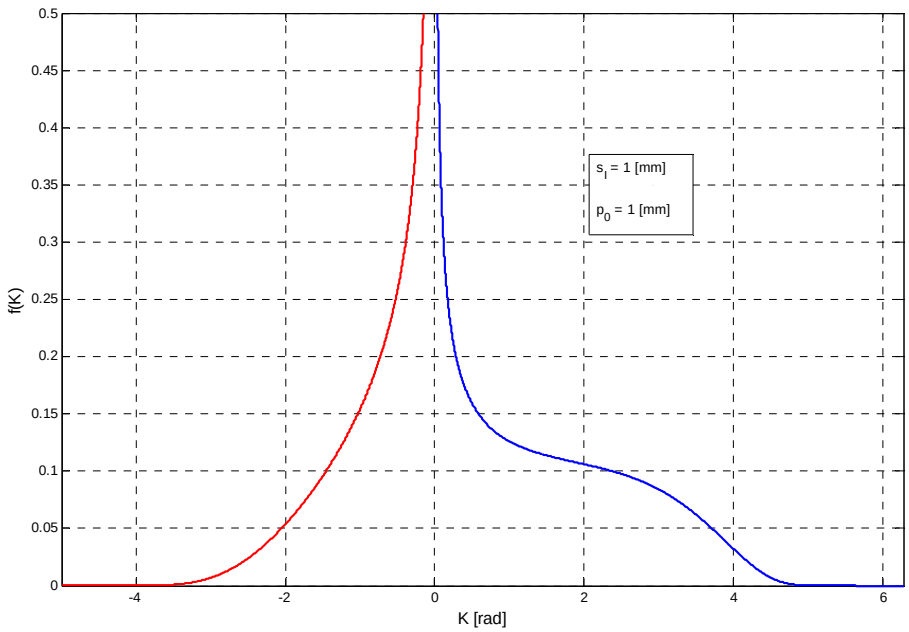

b)

Figure 7: probability density functions; a) normal distribution for "disturbance" along the *x*-axis; b) curvature distribution due to the presence of "disturbance".

Considering the classical definition for standard deviation and the bi-univocal influence between the deviations s_I (i.e. the one related to the *z*-axis "disturbance") and s_K (i.e. the one related to the curvature distribution), which has been verified by means of some experimental tests, it is possible to obtain:

$$s_K = \sqrt{s_K^2} = \sqrt{\int_{-\infty}^{+\infty} f(K)\cdot\left(K-\mu(K)\right)^2 dK} = \sqrt{\int_{-\infty}^{+\infty} f(K)\cdot K^2 dK} = s_K\left(s_I\right). \tag{11}$$

Finally, it is relevant to point out that the pitch function can also be directly derived from the discrete curvature parameter:

$$p = I\sqrt{\frac{1-\cos\left(\frac{2\pi-K}{4}\right)}{\cos\left(\frac{2\pi-K}{4}\right)}} = s_I\left(s_K\right)\sqrt{\frac{1-\sin\left(\frac{K}{4}\right)}{\sin\left(\frac{K}{4}\right)}} = p\left(K, s_K\right) \tag{12}$$

In particular, having regard to the normal distribution assumptions about the "disturbance" statistical behaviour, the pulse intensity along the z-axis I can be replaced by the standard deviation s_I. Considering the classical extended uncertainty formula

$$I(t\%) = \mu_I \pm k(t\%)\cdot s_I \tag{13}$$

it is possible to know which are the boundary conditions for the I existence after a specific coverage factor k has been selected. Besides, it is important to notice that in this formula, k is related to the t confidence level. Thus, equation (13) describes the boundaries of a range, with bilateral error risk $e = 100 - t\%$, that contains all the values assumed by I. Hence, if the variation interval for the random variable I were assumed with the following confidence level

$$I(99{,}73\%) = 0 \pm 3\cdot s_I = \pm 3\cdot s_I \tag{14}$$

but, if the equation were assigned a lower confidence value

$$I(68{,}27\%) = 0 \pm s_I = \pm s_I \tag{15}$$

I could be replaced by $s_{i.}$ Furthermore, as it has been previously explained, the standard deviation s_I can be linked to the parameter s_K, whose estimator can be directly calculated from the curvature map as a sample standard deviation. Hence, the resulting pitch function value can be easily calculated for every point of the cloud. This function shows dependence not only on the curvature value associated with each point, but also on the global statistical characteristics of the Gaussian curvature distribution (i.e. its estimated standard deviation s_K) which have been sampled all over the original surface. The whole set of the optimal pitch values proposed constitutes the so called "pitch map". The main purpose of this "pitch map" is to determine which resolution is the most suitable to be used during the acquisition process of each surface zone. This choice is made depending on the local morphological complexity, which has been previously measured through curvature analysis.

3.3 influence of the curvature distribution (s_K) on the pitch function

The pitch function (12) has been calculated for the positive values of the K curvature, and it has shown dependence on the K parameter itself and on the standard deviation s_K . An example of family of pitch functions, generated by assuming different values of s_K, is provided by the graph in figure 8 .

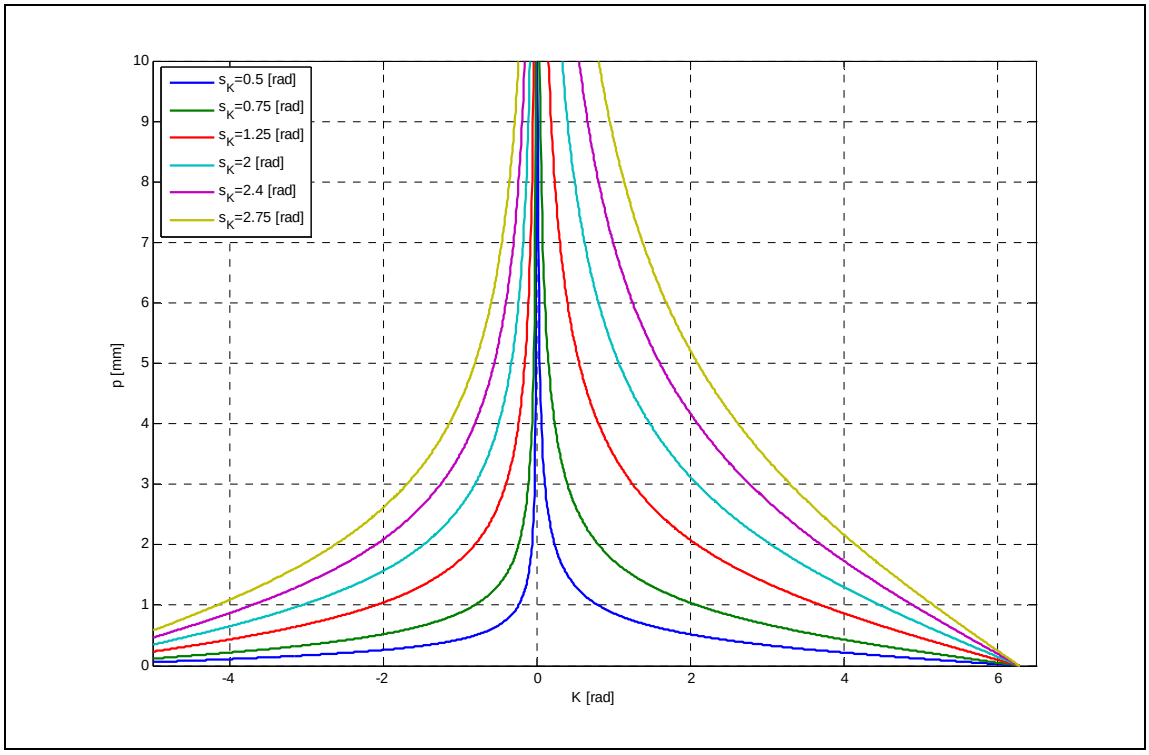

Figure 8: influence of curvature distribution s_k on a pitch function

If the standard deviation s_K tends to zero, the corresponding function seems to collapse on the Cartesian axes. As mentioned before, the expected values of the curvature distribution always tend to zero; thus, a small standard deviation indicates the absence of relevant curvature values, i.e. a plane-like geometry. Such a surface is assumed to be very regular; as a consequence, any sort of noise, no matter how slight, will have a strong effect on the local surface interpretation. For this reason, as it is shown in figure 8, the analysis of such a surface will suggest to use very small pitch values to scan those areas characterized by relatively small curvature amounts.

On the other hand, a higher value for the standard deviation s_K means that the considered surface is quite different from a simple plane, and that the "disturbance" is preponderant. In this latter case the function tends to assume a linear shape, with enhanced inclination. Therefore, in this case, the surface analysis will suggest to use high pitch values even in presence of relatively high curvature amounts.

In other words, the values assumed by the standard deviation s_K determine the pitch function sensitivity to "disturbance". If the estimated standard deviation is small, then the corresponding pitch function will prove to be optimal for very smooth surfaces, e.g. plane-like ones. Any sort of anomaly, even a small one - such as roughness, needles, edges etc. - will be seen as an interesting area for pitch strong reduction.

However, it must be pointed out that if the standard deviation amount is not negligible, the resulting

pitch function shall be adjusted based on the presence of "disturbance". This means that anomalies under a certain threshold shall not be considered as affecting the surface features; hence a relatively large pitch will be adopted in spite of their presence (Fig.9).

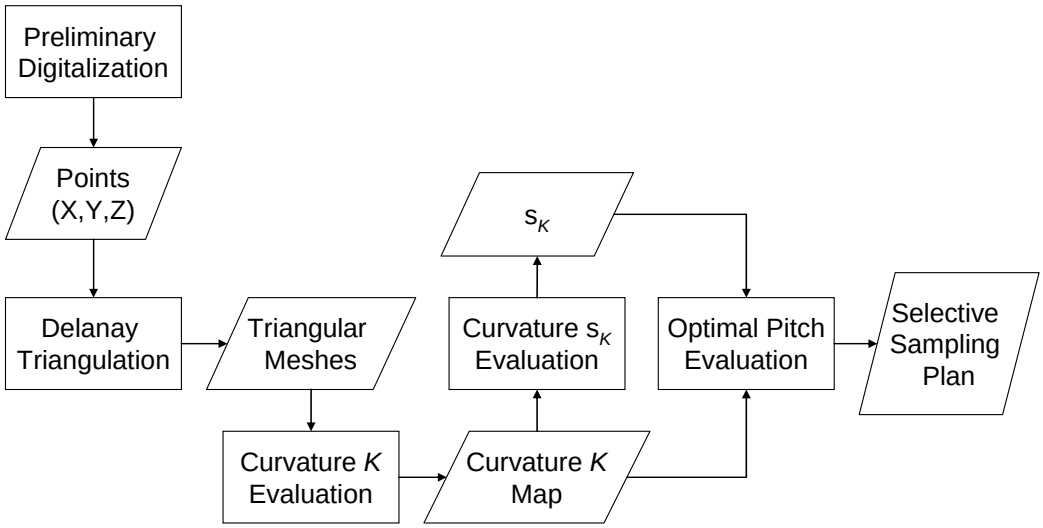

Figure 9: methodology flowchart: both geometrical and statistical analyses of the curvature start from a preliminary point cloud investigation. The optimal pitch function is then obtained from the curvature map, thus allowing direct point cloud improving

4. Pitch map design methodology validation

The approach presented in this paper is to be applied during the acquisition phase and is based on a preliminary point cloud, thus it does not require the creation of any intermediate model. Besides, it suggests a precise strategy to obtain an optimal scanning plan by removing redundant points and by acquiring new points where the original surface has proved to be morphologically too complex. Thanks to the presence of the disturbance factor and of the s_k parameter, this method is able to automatically manage the point density distribution as well as the pitch function, without neglecting the specific acquisition scenario (geometry acquired, 3D scanner device, …). In fact, as mentioned before, this method allows the finding of high pitch values even when disturbance is significant and curvature amounts are relatively high. Small pitch values will be suggested only to scan "regular" surfaces, i.e. areas with relatively small curvature amounts.

Most of the older methodologies have had problems to figure out which point density better suits the local morphological complexity; as a result, they are not able to automatically modify their pitch function depending on the specific acquisition scenario. Most of the times, they are able to determine the optimal point density only after a specific deviation is provided. However, in order to assure that the standard of the performances provided by the methodology here described is at least as high as that of the performances obtained through the use of the already available methodologies, it has been decided to evaluate how much the pitch function of the new methodology differs from those of the other standardised methodology making a connection between a continuous model and a discrete one.

The standardised methodology selected in order to carry out this test has been the STL one (Fig.10), i. e. the total deviation approach. This approach has been chosen because of its ability to provide different point

densities depending on the curvature evaluation, [13] and also because, at present, it is considered as the standard method within the CAD context.

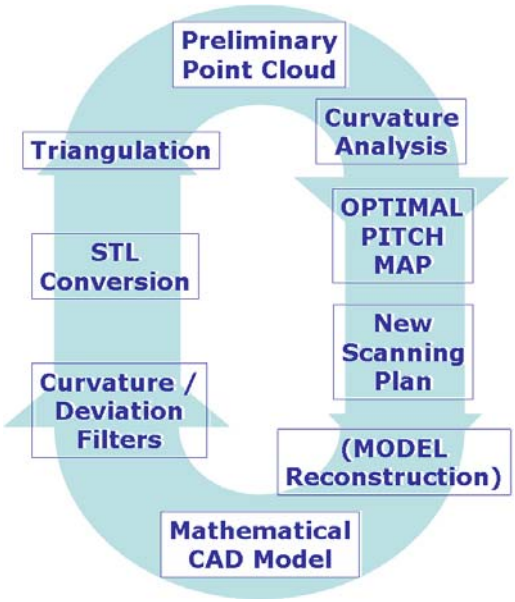

Figure 10: STL file generation and selective sampling approach

As shown in figure 11a, the two functions do not reasonably differ

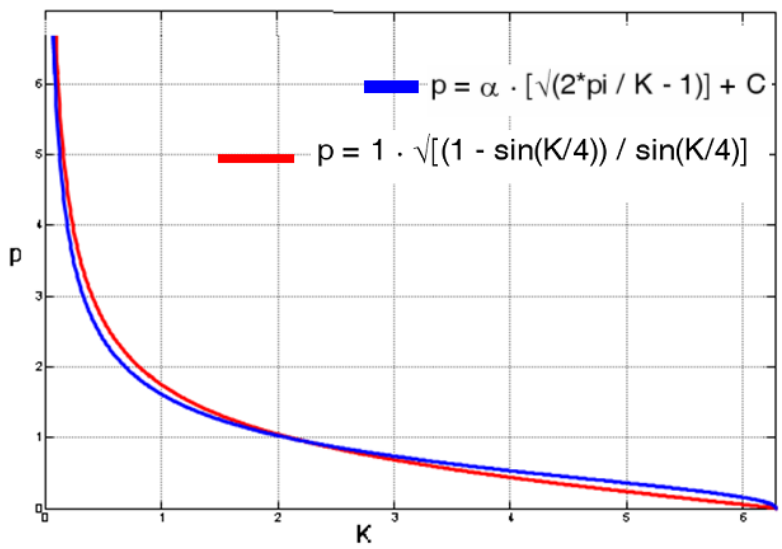

(a)

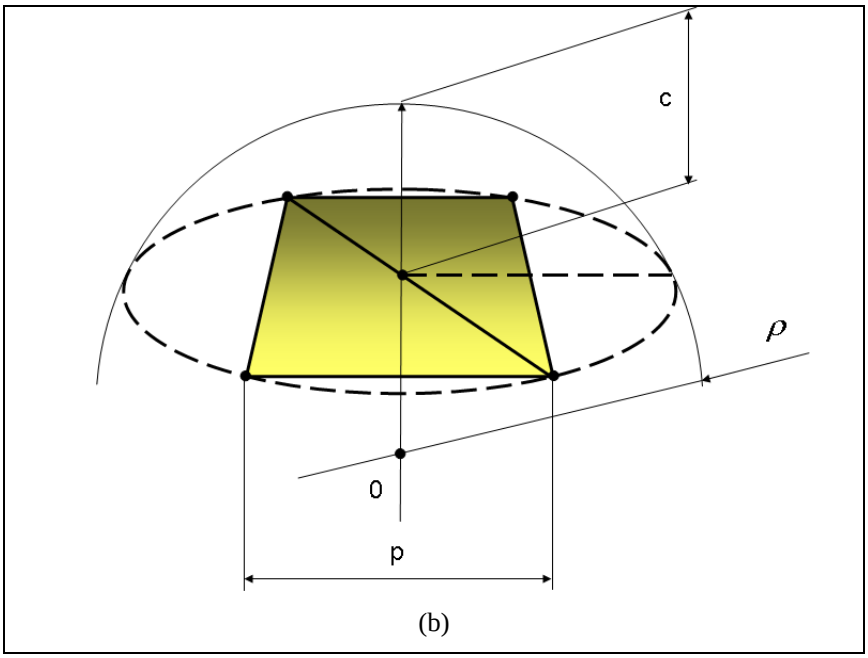

Figure 11: a) pitch function comparison; b) STL generation approach (total deviation method); *c* represents the deviation amount between the original surface (white) and the approximating triangulation (yellow)

Another, more practical proof of the efficiency of the approach hereof has been obtained by analysing a benchmark surface. In particular, the knowledge of the CAD model will render it possible to:

- generate a Cartesian-structured scattered grid for preliminary approximation, in order to be able to apply the approach here proposed and to heed the suggestions about point adding and removing;

- directly convert the continuous CAD model through STL file generation routine, in order to heed the approximate dimensions of each triangle as well as the local nodes' density provided by the STL grid.

The chosen benchmark surface is represented in figure 12. When looking at figure 13, it is possible to observe that the two outcomes are rather similar: this constitutes an important proof of the efficiency of the new approach here proposed.

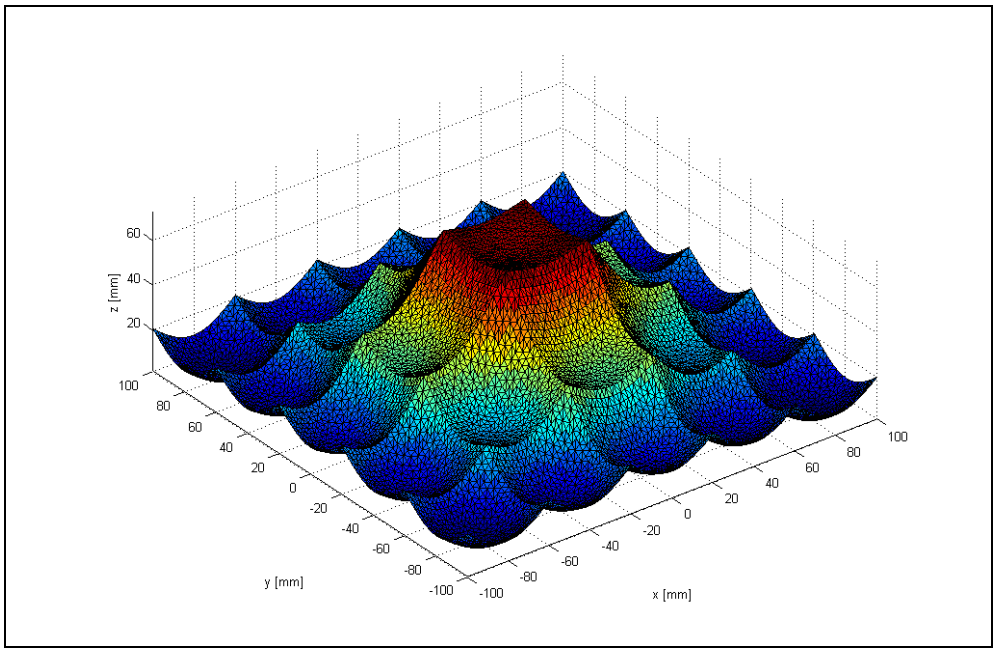
z [mm]
60
40
20
100
80
60
40
20
0
-20
-40
-60
-80
-100
y [mm]
-100
-80
-60
-40
-20
0
20
40
60
80
100
x [mm]

a)

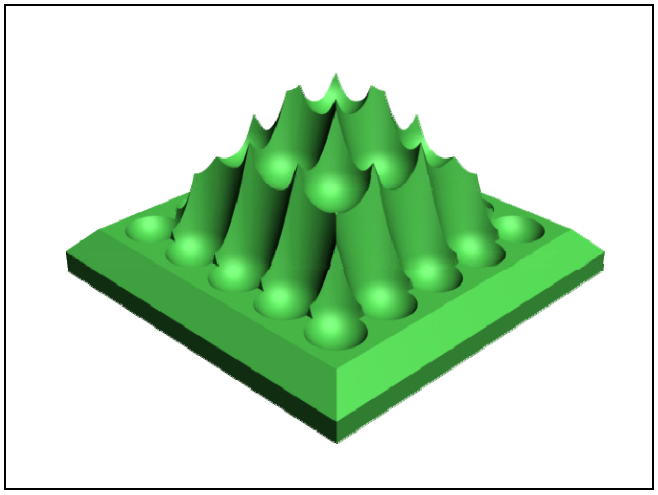

b)

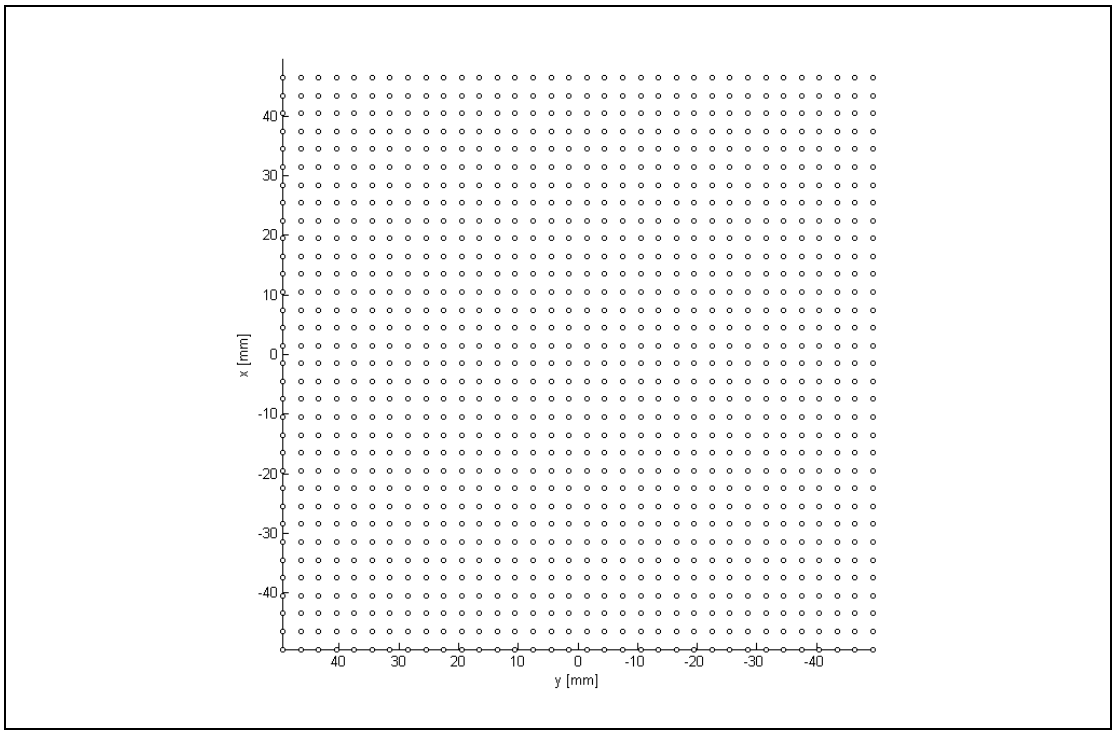

c)

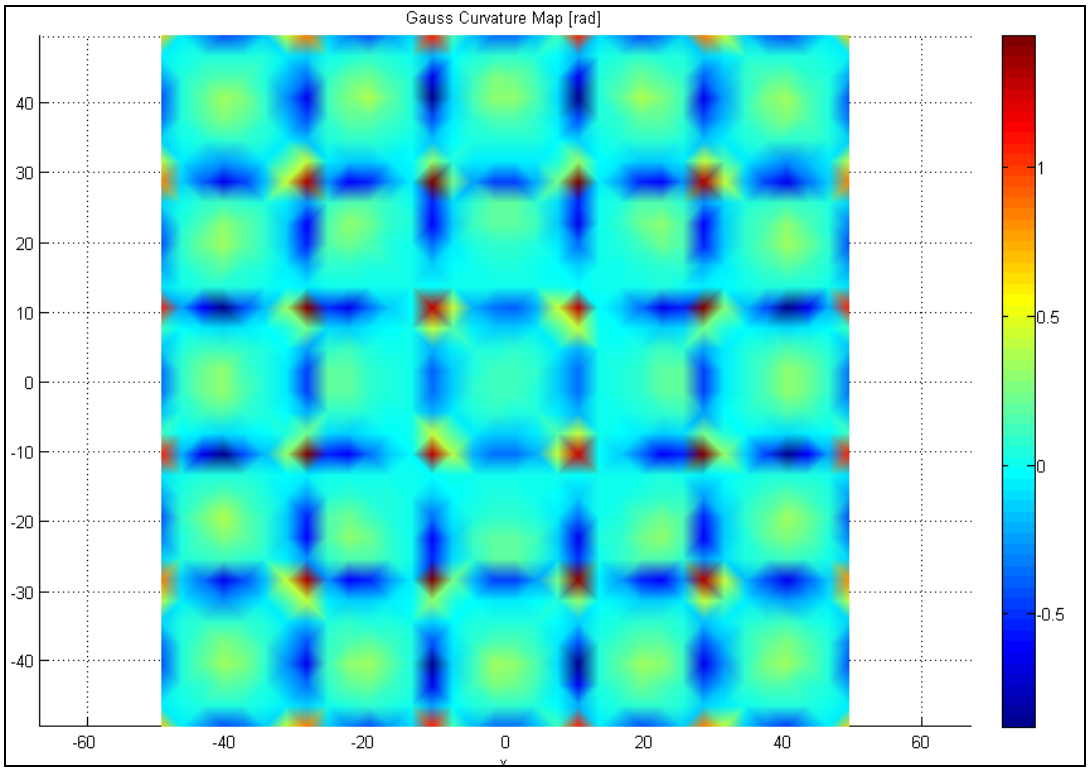

d)

Figure 12: benchmark surface: a-b) mathematical/CAD model; c) simulated preliminary point cloud; d) curvature map for the preliminary point cloud.

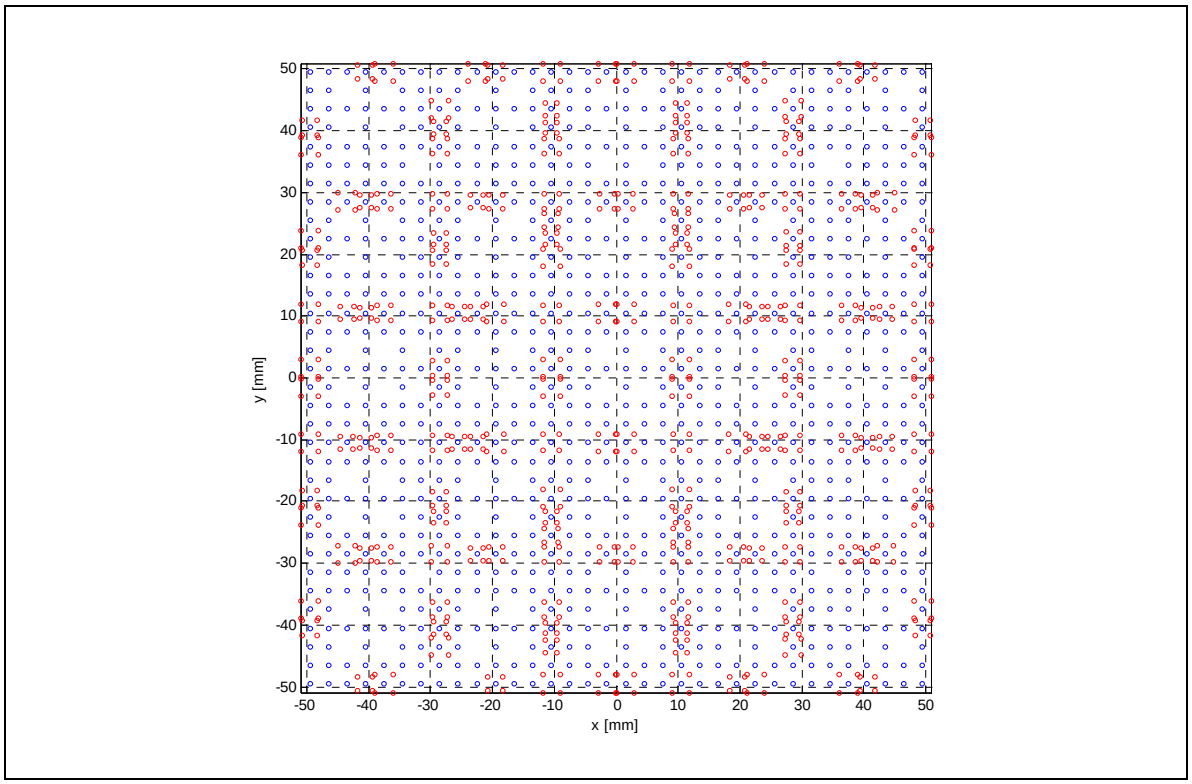

a)

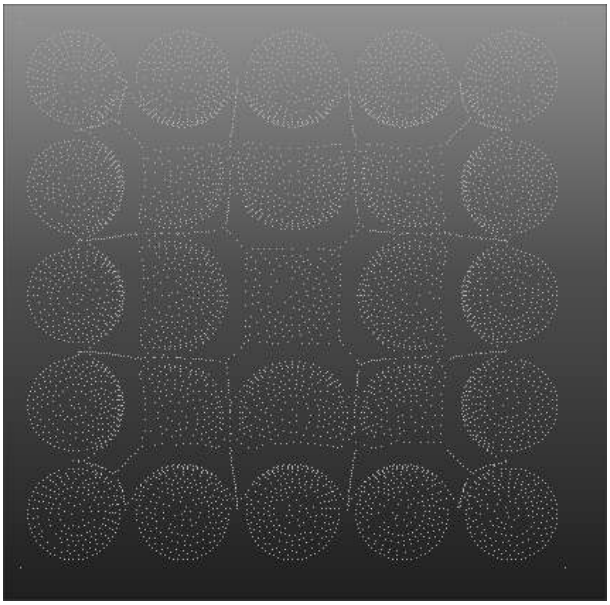

b)

Figure 13: benchmark surface; a) optimal pitch map, obtained from curvature analysis; b) STL triangulation

The approach here proposed aims at improving the point cloud density through curvature map analysis and pitch map generation. In order to verify its efficiency and reliability under more realistic conditions, this approach has been applied to several different scanned surfaces, always starting from a homogeneous, arbitrary scanning grid. This experimental validation has been implemented by employing two different 3D scanner devices, characterised by different performances (acquisition precision, accuracy and points clouds dimensions) and by six different geometries, some of which with smooth features while others with irregular ones. The object of this validation has been the simulation of a wide range of different possible scenarios in which the (proposed) methodology here proposed could possibly be used .

The first experiment has been carried out on a real facial profile (Fig.14), that is on a surface characterised by smooth behaviour and by some natural irregularities (skin, beard,…). This sample surface has been acquired by using an optical 3D scanner device (Minolta VIVD 900 [14]).

After the application of the algorithm, the point cloud has shown a significant decrease in points' density decrease. By working with the preliminary point cloud data (it is important to point out that, due to the precision and resolution of the 3D scanner employed, these data showed very few significant irregularities), the algorithm has suggested to limit the use of a high points' density only to those areas of the face which exhibited significant anatomical anomalies (eyes, nose, mouth) (Fig.13d).

As far as the second experiment is concerned, the surface used to carry it out has been again a human face (Fig.14). This time, the object has been acquired by using a contact piezoelectric device (i.e. a Roland Picza [15]), in order to test the proposed algorithm over both contact and non contact devices. More in detail, the originally scanned surface was a plaster calc of an artificial human face previously modelled: that is why most of the "disturbance" sources related to skin, nose and eye imperfections which appeared in the previous test, did not appear in this one. Considering that the 3D scanner used was more precise and that the face here employed was just the simulation of a real one (i.e. it had no natural irregularity), it is possible to conclude that the algorithm has provided a points' density distribution similar to the one yielded by the previous test. In fact, the density here suggested tends to be high around the most significant facial features, while it is rather low on the other areas. Taking into account that in this experiment the preliminary selected pitch was higher than the one used in the first test, it is quite easy to understand that both in-fitting and de-fitting operations have been involved.

These first two experiments have shown that the algorithm presents a reliable behaviour, i.e. it evidences only the relevant geometrical features of the acquired surface, both working with contact or non contact devices and despite the changing of the preliminary acquisition pitch.

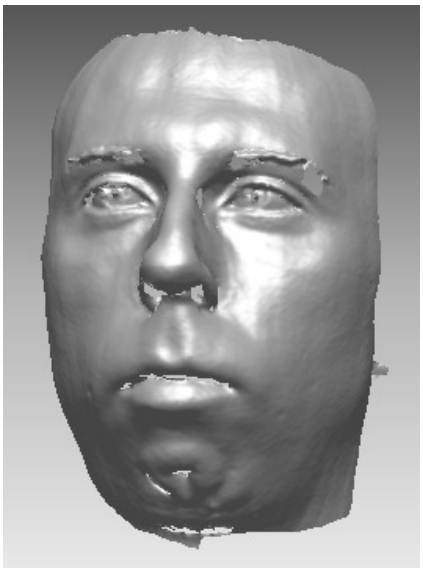

(a)

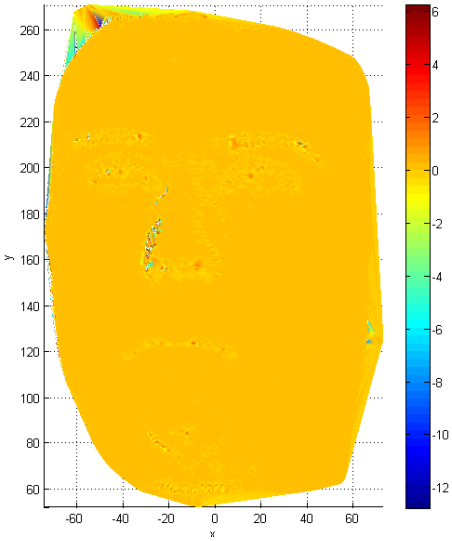

(b)

Preliminary Scanning

Pitch: 0,8mm

Original Points

Number: 53506

New Proposed Points

Number: 7281

Main improvement:

De-Fitting

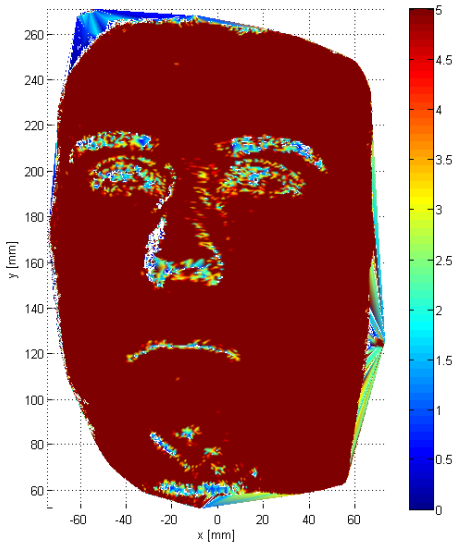

(b)

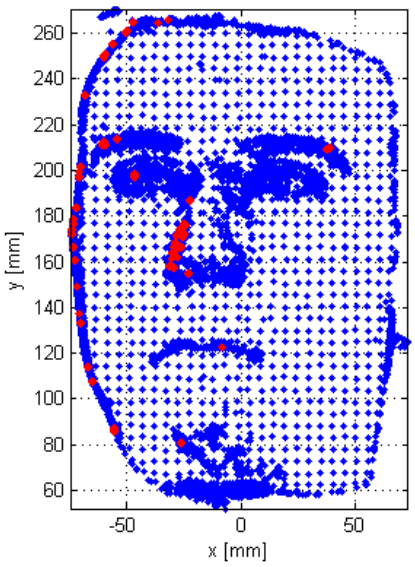

(d)

Figure 13: curvature analysis and optimal pitch calculation; a) preliminary view; b) curvature map; c) pitch map; d) improved local points' density.

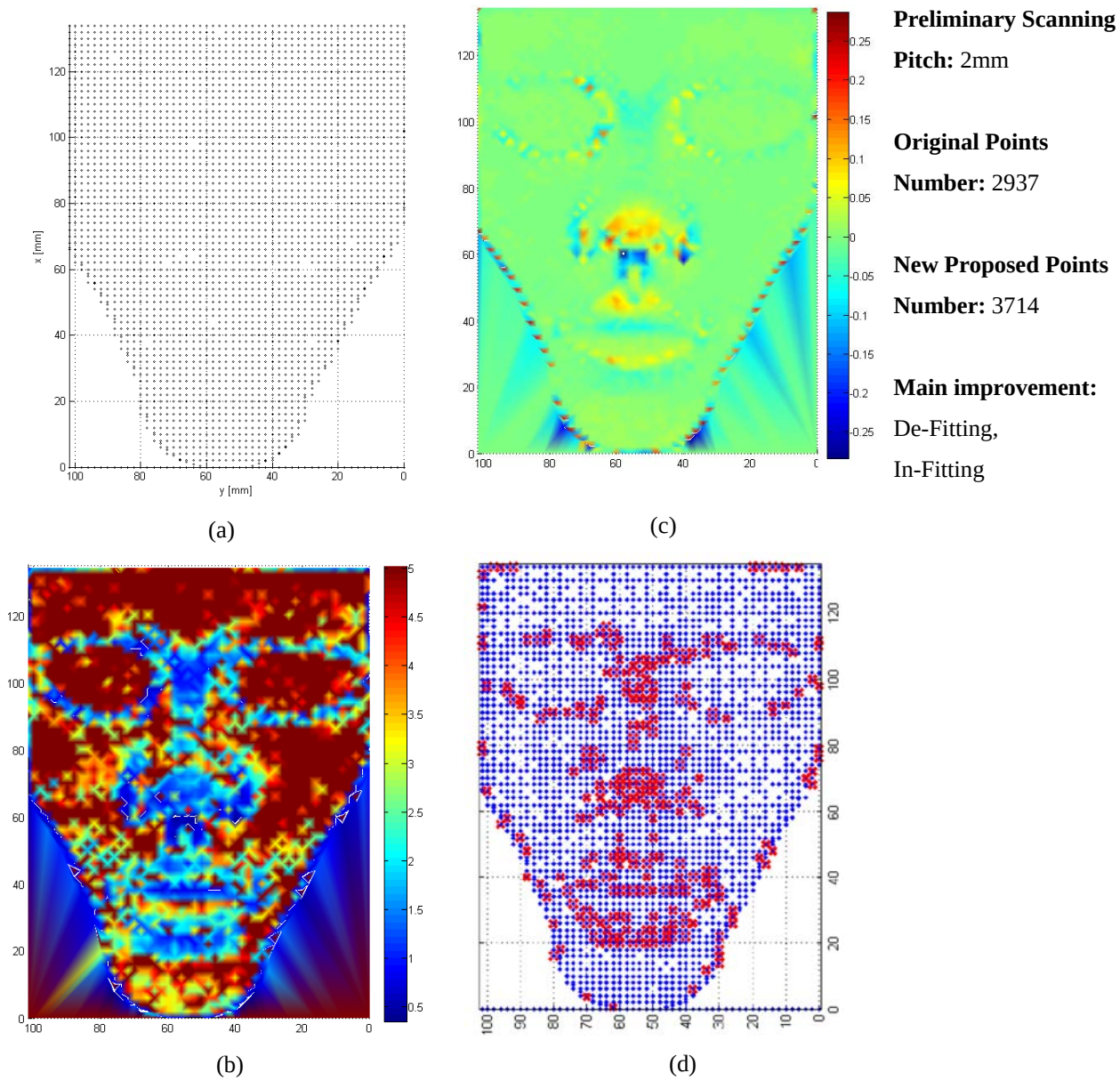

Preliminary Scanning Pitch: 2mm

Original Points Number: 2937

New Proposed Points Number: 3714

Main improvement:
De-Fitting,
In-Fitting

Figure 14 : curvature analysis and optimal pitch calculation; a) preliminary view; b) curvature map; c) pitch map; d) improved local points' density.

The third experiment (Fig.15) has again been carried out with the Roland device and it concerns the enlarged reproduction of a jewel. Even though the object in question is characterised by the presence of a quite smooth behaviour, the number of points does not change significantly before and after the algorithm application. In this situation the methodology has suggested a significant redistribution of the point locations.

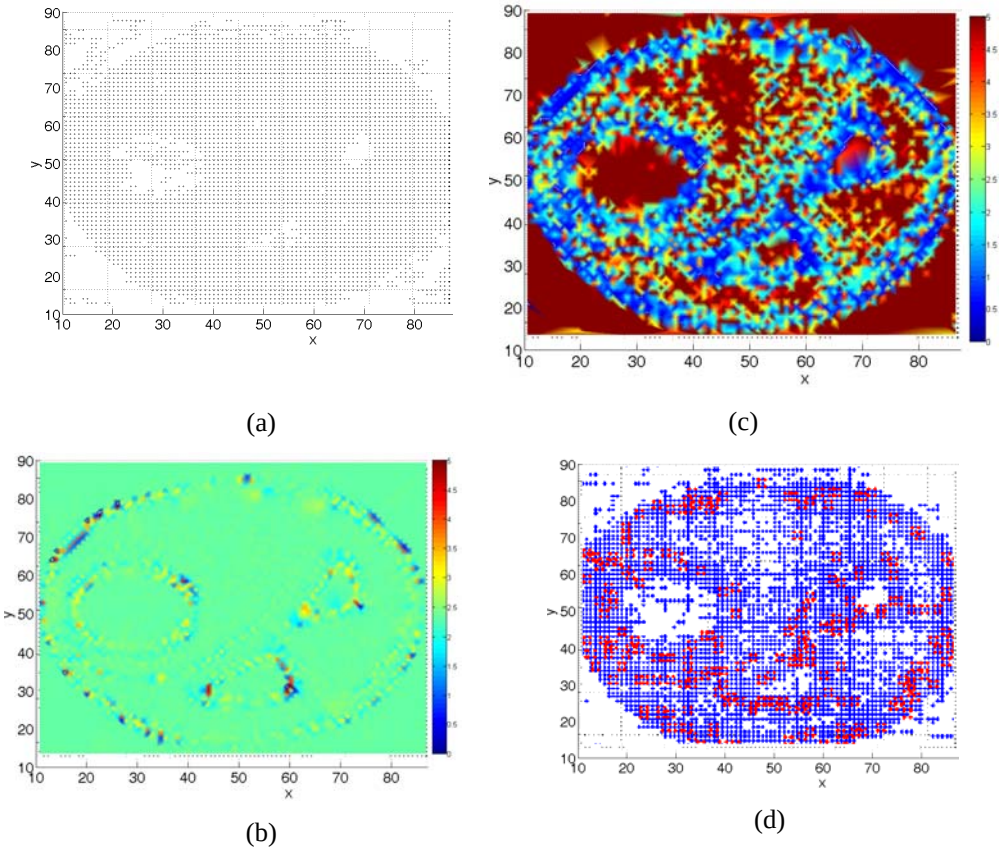

Preliminary Scanning Pitch: 1,6mm

Original Points Number: 4943

New Proposed Points Number: 4930

Main improvement: De-Fitting, In-Fitting

Figure 15: curvature analysis and optimal pitch calculation; a) preliminary view; b) curvature map; c) pitch map; d) improved local points density.

The next case (Fig.16) concerns a resin reproduction of a jewel which has been acquired through the same contact device. Here the "disturbance" effect is enhanced by the presence of sharp edges, holes and tips. If compared with the previous test, the disturbance value is here significantly higher. For this reason, the algorithm suggests to increase the points' density only on those regions where the curvature is high, while, as to the other regions, it recommends to adopt a more scattered points' distribution.

Both the third and the fourth tests have been carried out by using the same 3D scanner and similar pitch values, but employing two geometries with different disturbance values. By comparing the results yielded by these two tests, it is possible to notice that the algorithm ends up proposing two different point cloud distributions; besides, a stronger point cloud reduction tends to be suggested disturbance is higher.

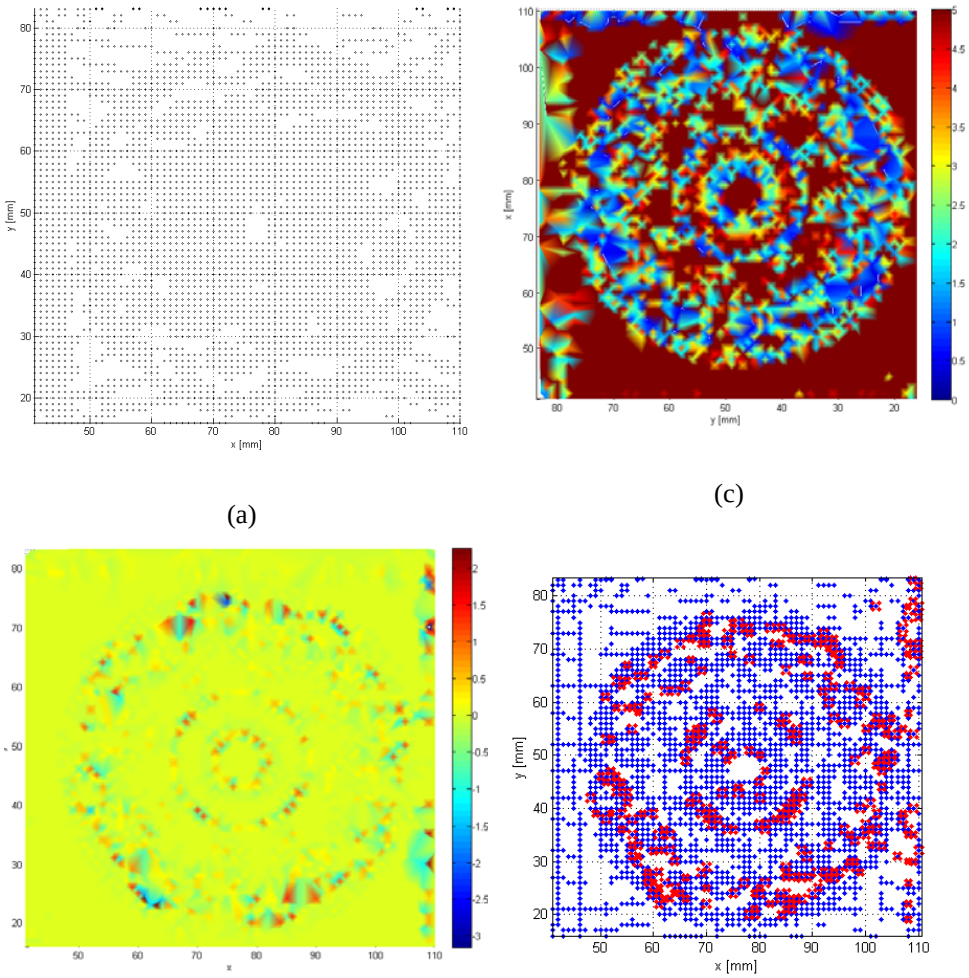

(a)

(c)

(b)

(d)

Preliminary Scanning Pitch: 1,4mm

Original Points' Number: 3683

New Proposed Points' Number: 3827

Main improvement:
De-Fitting,
In-Fitting

Figure 16: curvature analysis and optimal pitch calculation; a) preliminary view; b) curvature map; c) pitch map; d) improved local points' density.

As to the last two tests, other two different human faces (Fig.17) have been employed. In the fifth experiment, the Minolta optical device, which has been used to conduct the preliminary acquisition, has led to overcrowded point clouds, which have then been strongly lightened trough a series of de-fitting operations.

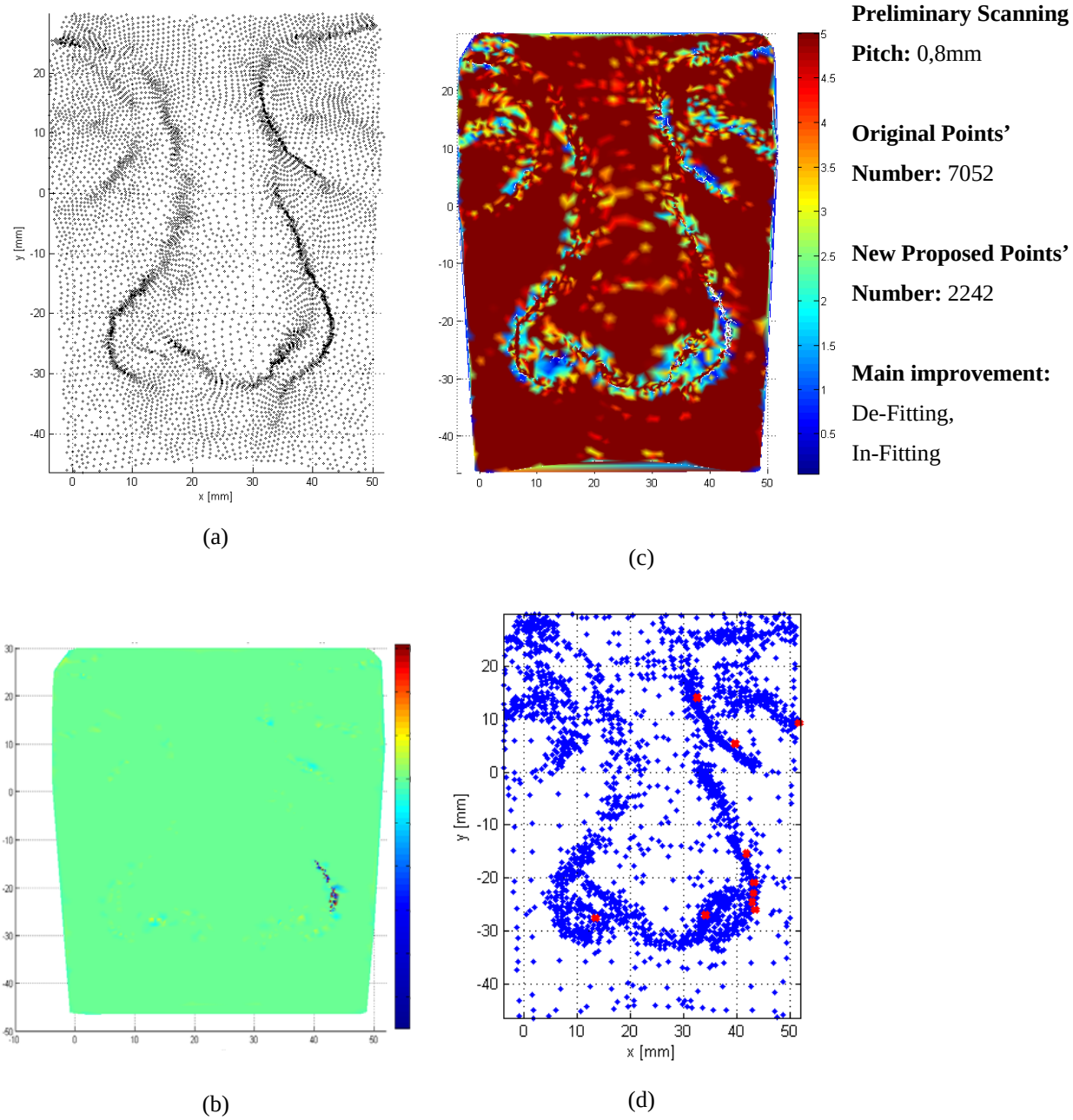

Figure 17: curvature analysis and optimal pitch calculation; a) preliminary view; b) curvature map; c) pitch map; d) improved local point density.

As the previous ones, even the last of the experiments here described has been carried out on a human face (Fig.18), which again has been acquired by using an optical scanning device.

Both the fifth and the sixth tests have been conducted by using the same optical 3D scanner; however, they have been carried out on two different faces. By comparing the results yielded by the of these two tests, it is possible to notice that in the latter one, where the face has a significant smooth behaviour, the algorithm proposes to reduce the points' density because the disturbance effect is quite negligible and the points' density is quite high. On the other hand, in the fifth test where the facial profile was characterised by many more descriptive features, only those regions with a high curvature value have shown a high point density.

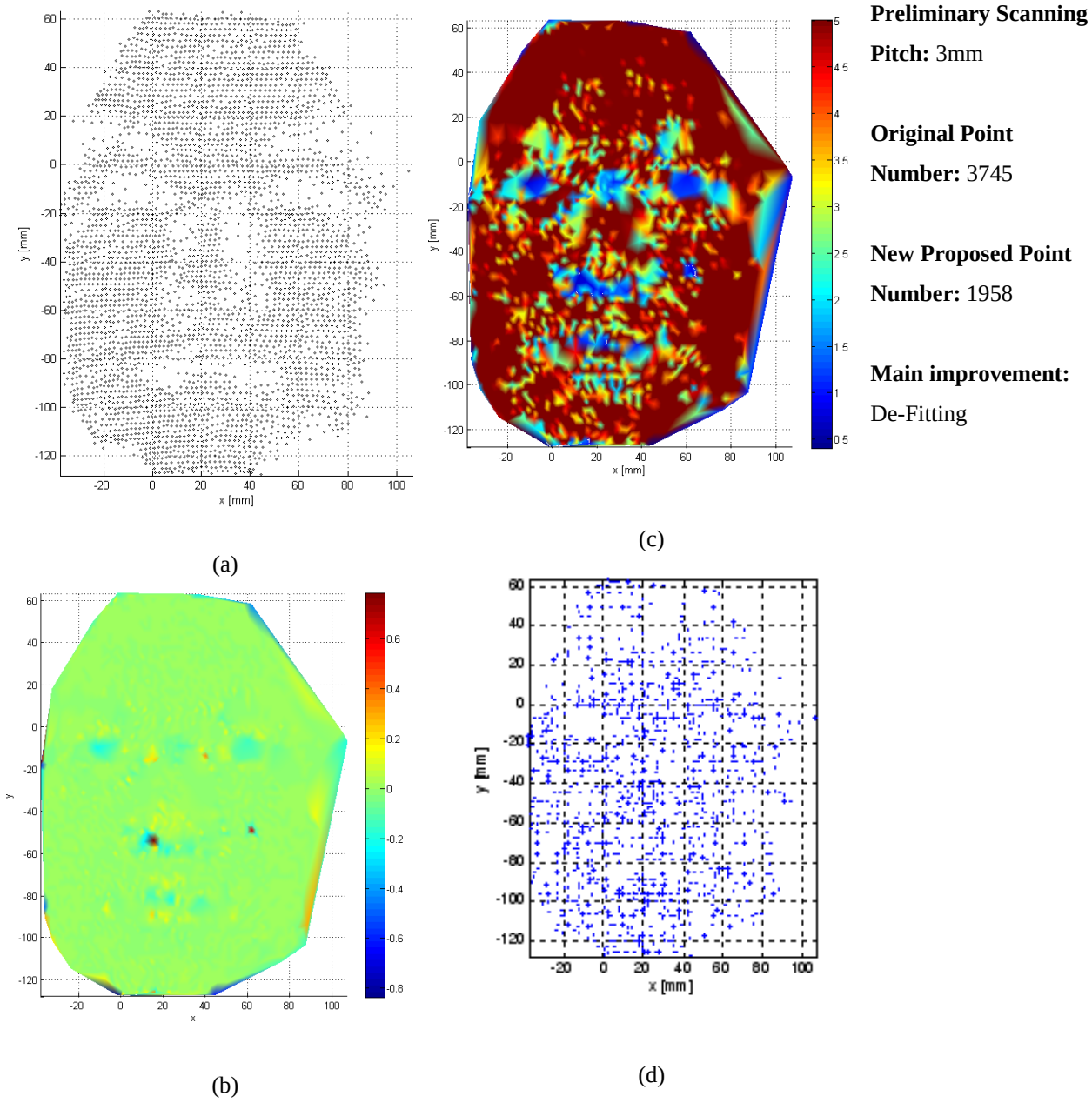

Figure 18: curvature analysis and optimal pitch calculation; a) preliminary view; b) curvature map; c) pitch map; d) improved local points' density.

The results yielded by the above mentioned experiments show that, when working with the same device, the algorithm here proposed is able to provide reliable point densities depending on the global morphological behaviour of the scanned object. In general, if the geometry is globally smooth, the algorithm will suggest to use a low pitch also for those regions with relative low curvature. On the contrary, if the surface exhibits many significant morphological features, a high points' density will be suggested only for the most significant ones.

6 Conclusions

This paper aims at proposing an innovative approach for designing optimal scanning grids. In particular, the

proposed methodology is based on an initial raw point cloud and has been designed through the evaluation of the discrete curvature value of each node (or neighbourhood). This new approach has been developed in order to provide an overview of the surface morphological complexity behaviour. Furthermore, this paper has introduced some innovative considerations about the definition of "Free-Form" surfaces: in fact, the previously mentioned scanned surfaces have been codified as "quasi-Free-Form" shapes, showing at least two contributions to morphological complexity. Moreover, the concept of "disturbance" has been explained in order to classify those uncertainties and noise effects introduced by the manufacturing process, the scanning device and sometimes even by the original CAD model itself (sharp edges, tips etc.). Experimental validations have then demonstrated that the so called "disturbance" often hides the true "free-form" ideal shape, as far as its contribution to the global morphological complexity is concerned. For this reason, the disturbance, which can be easily individuated, should be separately studied on the basis of mathematical and statistical models.

Since the optimal points' density within the cloud depends on the local morphology (which is represented by curvature nodal values and which is often driven by "disturbance") a further translation for the curvature control parameter has proved to be necessary. In fact, a direct value of a locally proposed new scanning pitch has been needed in order to efficiently improve the local point density of the clouds.

The "optimal pitch" function has been obtained from both geometrical and statistical considerations about the curvature behaviour over the whole examined surface. In fact, the family of the optimal pitch functions shows a strong dependence on the values assumed by the estimated standard deviation of the curvature population, i.e. s_K . In other words, since the expected value for curvature statistical distribution always tends to zero (at least as far as the examined surfaces are concerned), high values for s_K mean an increasing influence of the "disturbance" on the curvature behaviour of the whole surface. On the contrary, if even the deviation parameter s_K tends to zero, the considered manifold will probably tend to a "plane-like" ideal surface.

Thanks to the implicit presence of the deviation s_K in the optimal pitch formula, it is always possible to calibrate the translation of the curvature map into a pitch map by paying attention to the global statistical characteristics of the surface morphology. In particular, a pitch function calibrated by using a high deviation value will be less sensitive to small, sharp tips and to other noising features, e.g. roughness etc. In addition to pitch function defining, another important proof of the new approach effectiveness has been obtained by comparing the proposed technique with another, commonly used strategy for discrete models elaboration: the STL file generation, which is based on continuous CAD models and which is usually rendered possible by many CAD Suites.

In the last part of the paper, some particular application tests have been described. It is important to remember that these tests have been carried out, in order to analyse the proposed methodology behaviour. In particular, the analysis has focused on overcrowded point clouds (obtained from optical scanning devices) whose number of points has been significantly reduced. On the other hand, clouds with a rather high (or with a non too-low) preliminary scanning pitch value, showed both in-fitting and de-fitting improving of the local points' density.

In the same way, initial surfaces showing high values for the deviation parameter s_K, (i.e. strongly influenced by "disturbance") have proved to need both in-fitting and de-fitting operations.

In any case, any scanning plan obtained through preliminary point cloud elaboration, has shown an encouraging coherence between the new planned point position and the initial curvature map behaviour (i.e. the measured surface complexity).

Acknowledgments

The author wants to thank Mr. Alessio Courtial for the precious suggestions and help provided during the development of this research work

References

1. Varady T, Martin RR, Cox J. Reverse engineering of geometric models—an introduction. Computer-Aided-Design 1997;29(4):255–268
2. Bidanda B, Harding K., (1991) "Reverse Engineering: an Evaluation of prospective non contact technologies and applications in manufacturing systems", Int. J. Computer Integrated Manufacturing, Vol 30, No 10, pp.791 – 805.
3. Amenta, N., Bern, M., 1999. Surface reconstruction by Voronoi filtering. Discrete Comput. Geom. 22 (4), 481–504.
4. Ciarlet, P.G., Raviart, P.-A., 1972. General Lagrange and Hermit Interpolation in Rn with applications to the finite element method. Arch. Rational Mesh. Engrg. 46, 177–199.
5. Sarkar B, Menq C-H. Smooth-surface approximation and reverse engineering. Computer-Aided Design 1991;23(9):623–628
6. Weekenmann A, Eitzert H, Garmer M.,Weber H., Functionality oriented evaluation and sampling strategy in coordinate metrology, Precision Engineering 1995,17,244-252
7. K. Kase, A. Makinouchi, T. Nakagawa, H Suzuki, F. Kimura, Shape error evaluation method of free-form surfaces, Computer Aided Design 1999, 31; 495-505
8. Woo TC, Liang R., Dimensional measurement of surfaces and their sampling. Computer Aided Design 1993,25,233-239
9. K. Kase, A. Makinouchi, T. Nakagawa, H Suzuki, F. Kimura, Shape error evaluation method of free-form surfaces, Computer Aided Design 1999, 31; 495-505
10. Woo TC, Liang R., Dimensional measurement of surfaces and their sampling. Computer Aided Design 1993,25,233-239
11. Courtial, E. Vezzetti, New 3D segmentation approach for reverse engineering selective sampling acquisition, International Journal of Advanced Manufacturing Technology
12. G.Vicario, R.Levi, 1998, Calcolo delle probabilità e statistica per ingegneri, Progetto Leonardo, Bologna
13. Mortenson M. 1989, Geometrical Models in Computer Graphics, McGraw-Hill

14. Minolta VIVID 900 http://www.konicaminolta.com/

15. Roland Picza http://www.rolanddg.com